Sensor signals processing

Analytical Closed-Form Estimation of Position Error on ZUPT-Augmented Pedestrian Inertial Navigation

Yusheng Wang[1*], Daryosh Vatanparvar[1*], Andrei Chernyshoff[2*], and Andrei M. Shkel[1**]

[1]Department of Mechanical and Aerospace Engineering, University of California, Irvine, CA, 92697, USA
[2]Independent Consultant, Irvine, CA, 92603, USA
*Student Member, IEEE
**Fellow, IEEE

Manuscript received September 10, 2018; revised October 11, 2018; accepted October 30, 2018. Date of publication November 2, 2018; date of current version November 19, 2018.

Abstract—We present an analytical relation between the position estimation uncertainty and inertial measurement unit (IMU) characteristics during zero-velocity-update (ZUPT) augmented pedestrian inertial navigation. The effect of angle random walk of gyroscopes and velocity random walk of accelerometers in IMU on circular error probable is studied. Numerical simulation of the ZUPT-augmented navigation algorithm is conducted based on a generated pedestrian trajectory to verify the analytical results, showing the discrepancy less than 15%, which supports the fidelity of the results. Experiments are also conducted, and the results match our analytical prediction, with the error less than 20%. This study offers a closed-form analytical expression to predict the performance of ZUPT-augmented pedestrian inertial navigation.

Index Terms—Circular error probable, Kalman filter (KF), navigation error, pedestrian inertial navigation, zero-velocity update (ZUPT).

I. INTRODUCTION

The rapid development of microelectromechanical systems based inertial measurement units (IMUs) has made pedestrian inertial navigation possible, where the navigation is independent of preinstalled infrastructure, such as GPS, Wi-Fi, and LTE networks [1], [2]. It facilitates the pedestrian navigation in the environments where these signals are degraded or unavailable, such as indoor or underground. However, low-cost IMUs still suffer from high noise level and low stability; these effects accumulate during the navigation and result in significant navigation errors. For consumer-grade IMUs, for example, the position uncertainty will exceed a meter of error within just a few seconds of navigation [3].

A widely used compensation method for pedestrian inertial navigation is zero-velocity update (ZUPT) algorithm [4]. During the normal gait of human walk, the feet alternate between the stance and swing phases. Whenever the stance phase is detected, a ZUPT is applied in the ZUPT algorithm as pseudomeasurements in the Kalman filter (KF) to compensate for IMU biases, thus reducing the overall navigation errors. It has been demonstrated that velocity estimation errors can be bounded [5] and position estimation errors can be also greatly reduced, when ZUPT algorithm is implemented [6].

Although many studies have been conducted to demonstrate the effect of ZUPT algorithm on navigation errors, little work has been done to analyze the relation between the IMU performances and navigation accuracy in ZUPT-augmented inertial navigation. Angle and velocity estimation errors in ZUPT algorithm were analytically derived in [5], but the effect on the position estimation error was not reported. This article intends to fill the gap.

Corresponding author: Y. Wang (e-mail: yushengw@uci.edu).
Associate Editor: G. Langfelder.
Digital Object Identifier 10.1109/LSENS.2018.2879315

In this article, we first present a brief introduction of strapdown navigation with KF. Then, we analytically derive the position estimation error in ZUPT-augmented inertial navigation. Finally, the analytically derived closed-form estimation of position error is verified by both numerical and experimental results, showing the fidelity of the estimation.

II. STRAPDOWN NAVIGATION WITH KF

Standard strapdown inertial navigation system (INS) mechanization is implemented in the navigation frame, where the reference frame is fixed to the ground and its axes point toward north, east, and down directions. The attitude is defined by roll, pitch, and azimuth angles. The system states in the KF are the estimation errors, including the attitude, velocity, and position errors along the three directions [7]. After each estimation cycle, the KF would transfer the error estimation to the INS for navigation error compensation.

In this study, only angle random walk (ARW) of the gyroscopes and velocity random walk (VRW) of the accelerometers are considered. Other errors, such as long-term drifts, misalignments, and scale factor errors are neglected, as we assume they can be effectively estimated and compensated within KF using calibration algorithms. The transport rate is also neglected in our derivations.

For each time step, we propagate not only the estimation errors but their covariance matrix P_k for the following KF implementation as well. This is called the prediction step. In this study, P_k is expressed by 3×3 subblocks, representing angle, velocity, and position errors, respectively. When the stance phase is detected, ZUPT is applied, and velocity in the system state is considered as the measurement residual and transferred to the KF to update the state estimation. Velocity uncertainty is set in the range from 0.001 to 0.1 m/s [5]. As a part of the update step, the KF gain and covariance matrix are updated. Details of the KF implementation for ZUPT algorithm are reported in [4].

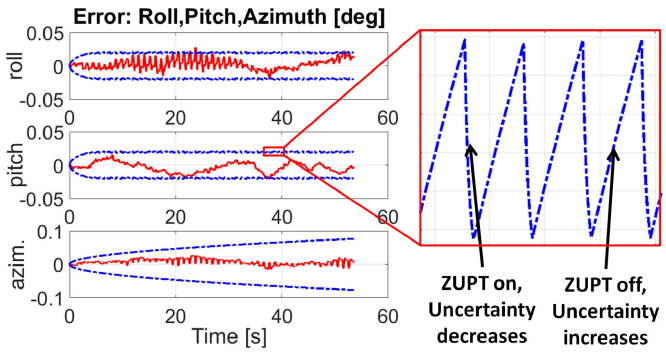

Fig. 1. Typical propagation of system state and its covariance in the KF.

III. NAVIGATION ERROR ANALYSIS

A typical propagation of the angle estimation error and its covariance are presented in Fig. 1. The red solid lines are the actual estimation errors, and the blue dashed lines are the 3σ uncertainty of estimation. Azimuth angle (heading) is the only important KF states that is not observable from zero-velocity measurements [8], and therefore, its uncertainty is proportional to the square root of the total navigation time as in the pure inertial navigation algorithms. Except for the azimuth angle, the system state uncertainty increases during the swing phase (ZUPT OFF) and decreases during the stance phase (ZUPT ON). The uncertainty reaches a constant level with some fluctuation after the initial transient stage, indicating that the uncertainty increase during the swing phase is equal to the uncertainty decrease during the stance phase. The former one is related to the IMU errors, and the latter one is related to the KF parameters, such as velocity uncertainty $\boldsymbol{w}_k$. In this approach, we combine the factors from both sides to estimate the overall performance of ZUPT-augmented inertial navigation.

Without loss of generality and for simplicity of analysis, in this study, we focus on a straight line trajectory toward north, neglecting any foot motion perpendicular to the trajectory.

A. Covariance Increase During Prediction Step

The subblock in the covariance matrix that corresponds to the position estimation error is P_{33}, and its propagation in the prediction step can be expressed as follows:

$$P_{33}^{\text{priori}} = P_{33} + (P_{23} + P_{32}) \cdot \Delta t + P_{22} \cdot \Delta t^2. \tag{1}$$

P_{23} and P_{32} are symmetric with respect to each other and share the same on-diagonal terms, and Δt is the time step. The last term on the right-hand side of (1) can be neglected since the sampling rate is high (typically around 100 Hz). The position estimation uncertainties along north and east are represented by $P_{33}(1, 1)$ and $P_{33}(2, 2)$, respectively, and they only depend on the propagation of $P_{23}(1, 1)$ and $P_{23}(2, 2)$, which correspond to coupling between the velocity errors and position errors. The propagations of the coupling terms are expressed as follows:

$$P_{23}^{\text{priori}}(1, 1) = P_{23}(1, 1) + [P_{22}(1, 1) - (g + a_D)P_{13}(2, 1)] \cdot \Delta t \tag{2}$$

$$P_{23}^{\text{priori}}(2, 2) = P_{23}(2, 2) + [P_{22}(2, 2) - (g + a_D)P_{13}(2, 1) + a_N P_{13}(3, 2)] \cdot \Delta t \tag{3}$$

where g is the gravity, a_N is the acceleration along north, and a_D is the acceleration toward down. The only difference between the two directions is the last term in (3).

Similarly, the propagations of other terms that will be used later are listed as follows:

$$P_{12}^{\text{priori}}(3, 2) = P_{12}(3, 2) + P_{11}(3, 3) \cdot a_N \cdot \Delta t \tag{4}$$

$$P_{13}^{\text{priori}}(3, 2) = P_{13}(3, 2) + P_{12}(3, 2) \cdot \Delta t. \tag{5}$$

B. Covariance Decrease During Update Step

Standard KF update is applied during this step. KF gain is first calculated, the estimation is compensated based on the measurement information, and then, the covariance matrix is also updated. The detailed derivation process is skipped due to the lack of space and only final results are presented as follows:

$$P_{13}^{\text{posteriori}}(3, 2) = P_{13}(3, 2) - P_{23}(2, 2) \cdot \frac{P_{12}(3, 2)}{w^2} \tag{6}$$

$$P_{33}^{\text{posteriori}}(1, 1) = P_{33}(1, 1) - \frac{P_{23}(1, 1)^2}{w^2} \tag{7}$$

$$P_{33}^{\text{posteriori}}(2, 2) = P_{33}(2, 2) - \frac{P_{23}(2, 2)^2}{w^2} \tag{8}$$

where w is the velocity measurement uncertainty. The main assumption in this step is that the propagated velocity covariance during the stance phase is much smaller than w. This assumption holds true because of a short time span of the stance phase.

C. Covariance Level Estimation

The detailed derivation is skipped due to the lack of space. Only a few important approximations are discussed here.

The propagation of $P_{12}(3, 2)$ is related to acceleration along north a_N and the azimuth angle uncertainty $P_{11}(3, 3)$, according to (4). In a single gait cycle, $P_{11}(3, 3)$ varies much slower than a_N. Thus, $P_{11}(3, 3)$ can be considered as constant, and $P_{12}(3, 2)$ is an integral of a_N, i.e., the velocity of IMU along north. Therefore, $P_{12}(3, 2)$ returns to near zero when the update step begins, and therefore, the update step has little effect on $P_{12}(3, 2)$ since its value is already close to zero. $P_{12}(3, 2)$ can be expressed as follows:

$$P_{12}(3, 2) \approx P_{11}(3, 3) \cdot v_N(t) = \text{ARW}^2 \cdot t \cdot v_N(t). \tag{9}$$

According to (6), the update step has also a little effect on $P_{13}(3, 2)$ since $P_{12}(3, 2)$ is close to zero during the update step. As a result, $P_{13}(3, 2)$ is an integral of $P_{12}(3, 2)$ according to (5), as follows:

$$P_{13}(3, 2) = \int \text{ARW}^2 \cdot t \cdot v_N(t) \cdot dt = \sum_i \int_{\text{cycle } i} \text{ARW}^2 \cdot t \cdot v_N(t) \cdot dt$$
$$\approx \text{ARW}^2 t_i \int_{\text{cycle } i} v_N(t) \cdot dt = \sum_i t_i \text{ARW}^2 s_N = \frac{1}{2}\text{ARW}^2 s_N t^2 \tag{10}$$

where s_N is the stride length of the human gait. In the approximation, t is considered as a constant during each gait cycle because v_N changes much faster than t in a single gait cycle.

The final expressions and central result of this article are as follows:

$$\sigma_{\parallel} = \sqrt{P_{33}(1,1)} = \sqrt{\left(2 - \frac{t_{\text{stride}}}{4}\right) \frac{t_{\text{stride}} w^2}{t_{\text{stance}} f} \cdot t} \tag{11}$$

$$\sigma_{\perp} = \sqrt{P_{33}(2,2)} = \sqrt{\left(2 - \frac{t_{\text{stride}}}{4}\right) \frac{t_{\text{stride}} w^2}{t_{\text{stance}} f} \cdot t + \frac{1}{3}\text{ARW}^2 s_N^2 \cdot t^3} \tag{12}$$

where $\sigma_{\parallel}$ and $\sigma_{\perp}$ are the position estimation errors parallel and perpendicular to the trajectory, and they correspond to 1.2 times of the semimajor and semiminor axes of circular error probable, respectively. A few observations based on the above equations are as follows.

1) The position uncertainty along the trajectory is dominated by the velocity measurement uncertainty w in KF and is proportional to square root of the navigation time. It is independent of IMU performance.
2) The position uncertainty perpendicular to the trajectory includes two terms. It is dominated by ARW and is proportional to the navigation time of the power of 1.5 in the case of long-term navigation.
3) VRW is not included in the equation. This is due to our assumption that the propagated velocity covariance during the swing phase is much smaller than the velocity measurement uncertainty w.
4) Higher sampling frequency helps reduce the position estimation uncertainty.

IV. VERIFICATION OF ANALYSIS

A. Numerical Verification

Simulations were conducted to verify the derived analytical expressions. First, a trajectory of foot toward north, and the corresponding IMU readouts were generated based on a human gait analysis [5]. Then, different levels of IMU noises were added to the readouts. Next, ZUPT-augmented inertial navigation algorithm was applied to the IMU readouts. The total navigation time of this numerical simulation was 107 s. VRW of accelerometers was set to be 0.14 mg/$\sqrt{\text{Hz}}$ (near tactical grade), velocity measurement uncertainty was 0.01 m/s, and ARW was swept from 0.01 to 10°/$\sqrt{\text{h}}$ (from near navigation grade to consumer grade).

Fig. 2 shows the relationship between the position uncertainty and ARW. A difference within 15% was demonstrated between the analytical results and the numerical results for relatively low ARW values. For higher ARW values, the assumption that the propagated velocity covariance during the stance phase is much smaller than the velocity measurement uncertainty does not hold good, and therefore, larger errors are expected.

B. Experimental Verification

A VectorNav VN-200 INS was mounted on the left shoe by a three-dimensional printed fixture (see Fig. 4), and IMU readouts were collected during walking. ARW and VRW of the IMU were 0.21°/$\sqrt{\text{h}}$ and 0.14 mg/$\sqrt{\text{Hz}}$, respectively [9]. Sampling frequency was set to be 800 Hz. The length of the straight trajectory was 200 m, and the total navigation time was 160 s.

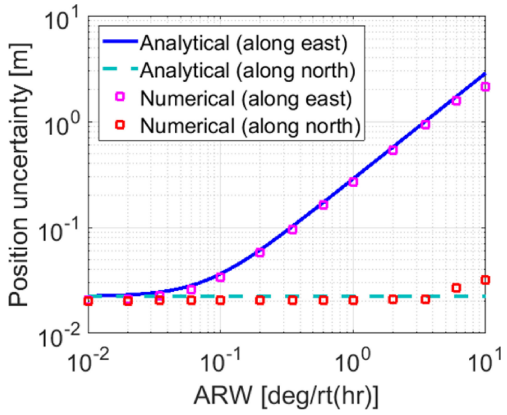

Fig. 2. Relation between ARW of gyroscopes and the position estimation uncertainties.

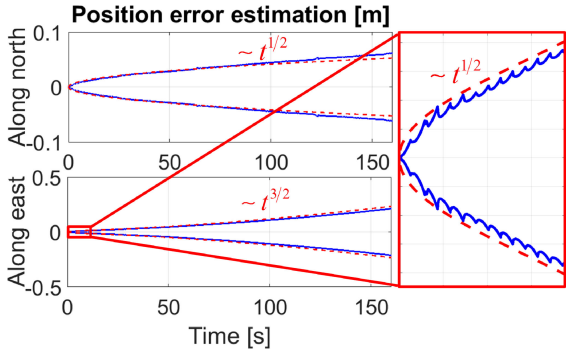

Fig. 3. Comparison between the analytical and experimental results for position estimation uncertainty.

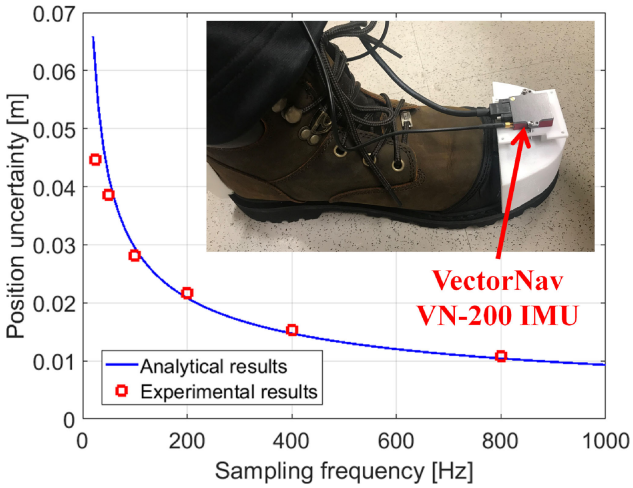

Fig. 4. Relation between the sampling frequency and the position estimation uncertainty.

The recorded IMU data were first processed to extract the position estimation uncertainty during navigation, and results were compared with analytical results from (11) and (12), as shown in Fig. 3. The red dashed lines are analytical results and the blue solid lines are experimental results. A difference within 20% was demonstrated. The position uncertainty along east is proportional to $t^{1/2}$ in the short term and is proportional to $t^{3/2}$ in the long term, well matching the analytical prediction in (12).

The same set of IMU data was postprocessed so that IMU readouts with different sampling frequencies were obtained on the same trajectory to study the relation between the uncertainty and the sampling frequency. The results are presented in Fig. 4. A close match has been demonstrated between the experimental results and analytical results with errors less than 10%. A relatively greater error at 25 Hz was possibly due to the effects of higher order terms with respect to Δt that were neglected in the derivation.

V. CONCLUSION

An analytical model predicting the position estimation uncertainty during the ZUPT-augmented inertial pedestrian navigation was derived for the first time. The analytically predicted position uncertainty was within 15% of both numerical simulation and experimental results. This article offers a closed-form analytical expression to predict the accuracy of ZUPT-augmented pedestrian inertial navigation.

ACKNOWLEDGMENT

This work was supported by the U.S. Department of Commerce, National Institute of Standards and Technology, under the financial assistance award 70NANB17H192. All work was conducted in the MicroSystems Laboratory at the University of California, Irvine.

REFERENCES

[1] X. Yun, E. R. Bachmann, H. Moore, and J. Calusdian, "Self-contained position tracking of human movement using small inertial/magnetic sensor modules," *IEEE Int. Conf. Robot. Automat.*, Roma, Italy, Apr. 10–14, 2007, pp. 2526–2533.

[2] A. R. Jimenez, F. Seco, C. Prieto, and J. Guevara, "A comparison of pedestrian dead-reckoning algorithms using a low-cost MEMS IMU," in *Proc. IEEE Int. Symp. Intell. Signal Process.*, Budapest, Hungary, Aug. 26–28, 2009, pp. 37–42.

[3] M. Ma, Q. Song, Y. Li, and Z. Zhou, "A zero velocity intervals detection algorithm based on sensor fusion for indoor pedestrian navigation," in *Proc. IEEE Inf. Technol. Netw. Electron. Automat. Control Conf.*, Chengdu, China, Dec. 15–17, 2017, pp. 418–423.

[4] E. Foxlin, "Pedestrian tracking with shoe-mounted inertial sensors," *IEEE Comput. Graph. Appl.*, vol. 25, no. 6, pp. 38–46, Nov.–Dec. 2005.

[5] Y. Wang, A. Chernyshoff, and A. M. Shkel, "Error analysis of ZUPT-aided pedestrian inertial navigation," in *Proc. Int. Conf. Indoor Positioning Indoor Navig.*, Nantes, France, Sep. 24–27, 2018.

[6] S. Godha and G. Lachapelle, "Foot mounted inertial system for pedestrian navigation," *Meas. Sci. Technol.*, vol. 19, no. 7, 2008, Art. no. 075202.

[7] D. Titterton and J. Weston, *Strapdown Inertial Navigation Technology*, 2nd ed., vol. 207. Reston, VA, USA: AIAA, 2004, pp. 402–409.

[8] A. R. Jiménez, F. Seco, J. C. Prieto, and J. Guevara, "Indoor pedestrian navigation using an INS/EKF framework for yaw drift reduction and a foot-mounted IMU," in *Proc. IEEE Workshop Positioning Navig. Commun.*, Dresden, Germany, Mar. 11–12, 2010, pp. 135–143.

[9] VectorNav VN-200, "GPS-aided inertial navigation system product brief, 2017. [Online]. Available: https://www.vectornav.com/docs/default-source/documentation/vn-200-documentation/PB-12-0003.pdf?sfvrsn=749ee6b9_13